Toxicology Reports 13 (2024) 101778

Contents lists available at ScienceDirect

Toxicology Reports

journal homepage: www.elsevier.com/locate/toxrep

Synthesis and evaluation of amyloid beta peptide/Ruthenium III-based complex drugs as drug delivery and anticancer activity

Rethinam Senthil [1]

Department of Pharmacology, Saveetha Dental College and Hospitals, Saveetha Institute of Medical and Technical Sciences (SIMATS), Saveetha University, Chennai, Tamilnadu 600077, India

ARTICLE INFO

Handling Editor: Prof. L.H. Lash

Keywords:
Amyloid beta peptide
Ruthenium III
Anticancer activity

ABSTRACT

The development and characterization of anticancer complex drugs (ACD), specifically Amyloid Beta Peptide (ABP) - Ruthenium III (Ru III) - nivolumab (NB), were explored through analytical techniques. Fourier-transform infrared (FTIR) spectroscopy demonstrated the structural transformation of peptides from α-helical to β-sheet formations, aligning with amyloid fibril aggregation. Ruthenium (III) complex synthesis was confirmed through distinct absorption peaks in FTIR analysis. High-resolution scanning electron microscopy (HRSEM) revealed the fibrous and smooth morphology of ACD, while thermogravimetric analysis (TGA) confirmed the decomposition stages and stability of the ruthenium complexes. The encapsulation efficiency and in vitro release profile of nivolumab (NB) within ABP-RuIII-NB were investigated, showing a two-phase release over 40 h. Cytotoxicity studies using acridine orange and ethidium bromide staining techniques indicated significant apoptosis in human oral squamous cell carcinoma (OSCC) -treated cells. These findings highlight the potential of ABP-RuIII-NB as an effective cancer treatment with controlled drug release and high cytotoxicity against cancer cells.

1. Introduction

Oral cancer, particularly oral squamous cell carcinoma (OSCC), is a major global health concern, with an increasing incidence rate. Despite breakthroughs in traditional therapies such as surgery, radiation, and chemotherapy, treating oral cancer presents substantial challenges, including drug resistance, recurrence, and severe side effects like mucositis and dysphagia [1,2]. Despite breakthroughs in traditional therapies such as surgery, radiation, and chemotherapy, treating oral cancer presents substantial challenges, including drug resistance, recurrence, and severe side effects like mucositis and dysphagia. This highlights the crucial need for innovative therapeutic approaches that not only improve treatment efficacy but also drug delivery selectivity to avoid off-target toxicity in the oral cavity [3].

Ruthenium-based complexes have emerged as intriguing options in cancer therapy due to their distinct chemical features, which include the capacity to perform redox reactions and form stable complexes in biological systems. Ruthenium (III) complexes, in particular, have shown strong cytotoxic effects on cancer cells, principally by targeting DNA and triggering apoptosis [4]. However, as with many metal-based medications, its therapeutic application in oral cancer has been limited due to concerns about poor selectivity and systemic toxicity. Recent research has proposed that conjugating ruthenium (III) complexes with biomolecules, such as peptides, could overcome these constraints by increasing the drug's stability, specificity, and delivery [5].

The continued search for effective cancer treatments has prompted extensive study into the creation of metal-based medications, notably those containing transition metals such as ruthenium (Ru) [6]. Ruthenium (III) complexes have shown exceptional potential as anticancer medicines due to their capacity to trigger apoptosis in cancer cells while being less toxic than typical platinum-based treatments like cisplatin. Despite these advancements, difficulties such as poor selectivity, low bioavailability, and multidrug resistance (MDR) continue to hinder the full therapeutic potential of ruthenium-based drugs [7].

This study's originality consists in the design and production of a ruthenium (III)-based compound conjugated with amyloid beta (Aβ) peptides, presenting an innovative approach to cancer treatment. Aβ peptides, formerly associated with neurodegenerative diseases like Alzheimer's disease, have shown potential in biomedical applications due to their ability to interact with cellular membranes and form structural scaffolds [8]. Aβ peptides can transport ruthenium complexes to cancer cells by targeting specific cell surface receptors, offering a

E-mail address: senthilbiop@gmail.com.
[1] ORCID: 0000-0002-3187-5673.

https://doi.org/10.1016/j.toxrep.2024.101778
Received 7 August 2024; Received in revised form 11 October 2024; Accepted 17 October 2024
Available online 18 October 2024

significant advantage in drug delivery [9].

This study investigates that combining ruthenium (III) complexes with amyloid beta peptides improves the drug's selectivity, stability, and efficacy in anticancer applications. The combination uses Aβ peptides' biocompatibility and affinity for cellular membranes to enhance medication administration and penetration in malignant tissues while reducing impacts on healthy cells. Additionally, the Aβ peptide acts as a scaffold, potentially improving the pharmacokinetics and biodistribution of the ruthenium complex.

The originality of this strategy extends to overcoming MDR in cancer cells. Amyloid beta peptides have been demonstrated to affect membrane integrity and impact cellular uptake routes, potentially increasing the intracellular accumulation of the Ru (III) complex and therefore amplifying its cytotoxic effects [10]. By synthesizing and testing this unique amyloid beta peptide/Ruthenium (III) complex, we want to create a drug delivery system that overcomes critical difficulties in cancer therapy, such as resistance mechanisms and off-target toxicity [11].

This study reports the first synthesis of an amyloid beta peptide/Ruthenium (III) complex with two functions: efficient drug transport and powerful anticancer action. The innovative usage of Aβ peptides enhances the therapeutic potential of Ru (III) complexes, offering a unique way to address the limits of conventional cancer treatments.

2. Materials and method

2.1. Preparation of amyloid beta peptide $_{(25-35)}$ - (ABP)

Amyloid Beta Peptide (25−35) is typically produced by dissolving the synthetic peptide in phosphate-buffered saline (PBS). The peptide is initially weighed and dissolved to a concentration of 1 mg/mL in PBS with a pH of 7.4 to help in solubilization. To improve peptide breakdown and decrease aggregation, sonication for 5–10 mins at room temperature is often used. Once dissolved, the solution is heated at 37 °C for 48 h to stimulate beta-sheet production, a step required for amyloid fibril aggregation. The produced peptide solution can then be aliquoted and kept at −20 °C for long-term use.

2.2. Synthesis of Ruthenium III (RuIII)

Ruthenium (III) complexes are commonly produced by reacting ruthenium chloride ($RuCl_3$ $3H_2O$) with appropriate ligands in a suitable solvent. In a typical procedure, ruthenium (III) chloride (0.06 M) is dissolved in ethanol and the ligand (3-amino-1, 2, 4-triazole (95 %), 1, 3-diphenylpropano-1, 3-dione (98 %), 6-methylheptane-2, 4-dione (98 %), 3, 5-heptanedione (98 %), hydrochloric acid (37 %), n-octanol (99 %), sodium chloride (99 %), and ethylene glycol)) is added stoichiometric amounts. The reaction mixture is agitated at reflux temperatures ranging from 60 °C to 80 °C for 8 h, allowing the complex to develop. After completion, the solution is cooled to ambient temperature and the solvent evaporates under reduced pressure. The resultant product is filtered and refined, usually by recrystallization of ethanol.

2.3. Development of anticancer complex drugs (ACD)

The anticancer complex drugs (ACD) were prepared using the surface activation method. 300 μL of NB was incubated in 4 mL of 0.2 M PBS containing 40 mg EDC and 8.5 mg NHS for 30 mins. To this, 10 mg of ABP and 5 mg of RuIII dispersed in 5 mL in distilled water was added and stirred for 5 h. After incubation, the mixture was ultracentrifuged for 3 times at 40,000 rpm for 20 min. To encapsulate NB, the drug was dissolved in ethanol and combined with the dried peptide-ruthenium complex, ensuring uniform distribution before evaporating the solvent under reduced pressure to form the ABP-RuIII-NB complex [12].

2.4. Physicochemical characterization

Fourier-transform infrared (FTIR) spectroscopy observations were conducted with a Nicolet 360 instrument. Thermogravimetric analysis was carried out with a high-resolution 2950 TGA (TA Instruments) in a nitrogen environment at a flow rate of 50 mL/min. The peptide sample, subjected to a pH 7, was incubated at 37 °C for 10 days with 5 mM Thioflavin T (ThT). The ThT stock solution was prepared using 50 mM glycine buffer. Fluorescence spectroscopy measurements were taken at various time intervals (0–24 h) using a Perkin-Elmer (LS-45) luminescence spectrometer. High-resolution scanning electron microscopy (HR-SEM) images were recorded using a 15 kV promoting voltage, 5 nm accuracy (Thermo Scientific Apreo S), and 5000× magnification.

2.5. Invitro drug release study

To measure the amount of NB trapped within ABP-RuIII, 5 mg of the sample was treated with 1 mL of PBS and 125 μL of DMSO. The mixture was vortexed for 10 minutes before being centrifuged at 10,000 rpm and the supernatant's absorbance was measured at 345 nm. The quantity of NB entrapped in ABP-RuIII was determined using the following formula: The entrapment efficiency is calculated as (NB in ABP-RuIII / NB initially used) times 100 %. To investigate the NB release profile, 2.5 mg of ABP-RuIII was put in a dialysis membrane bag (MWCO: 10,000 Da) with 1.5 mL of PBS (pH 7.4). Samples were collected at predefined intervals, centrifuged at 10,000 rpm, and measured for UV absorption at 345 nm. The quantity of the external phase buffer medium was kept constant by introducing 1.5 mL of the correct buffer solution. The volume of the outer phase buffer medium was maintained constant by adding 1.5 mL of a suitable buffer solution.

2.6. MTT assay

The cytotoxicity of NB-ABP-RuIII on oral OSCC cell lines was determined using the common MTT assay. A total of 1×10^5 cells were seeded into 96-well tissue culture plates and incubated overnight. The cell growth medium was then replaced with fresh medium containing NB-ABP-RuIII dispersion and incubated for 24 h. After this period, an MTT assay was performed to evaluate the cytotoxic effect of the compounds. To investigate cell death morphology, fluorescent DNA-binding dyes acridine orange (AO) and ethidium bromide (EB) were used. A total of 1×10^6 oral SCC cells were cultured in a 12-well plate and incubated for 24 h. The cells were then treated with the IC_{50} concentration of NB-ABP-RuIII for an additional 24 h. Post-incubation; the cells were stained with 10 μL of AO-EB solution (1 mg of AO and EB in 1000 mL of PBS) and observed under a fluorescence microscope (Olympus BX-51) [13].

3. Results and discussion

3.1. Characterization of ABP and Ru (III)

The FTIR analysis of ABP and RuIII are shown in Fig. 1(a&b). The ABP spectra initially showed a peak at ~1655 cm^{-1}, signifying α-helical structures. As aggregation progressed, this peak shifted, and additional peaks emerged at ~1625 cm^{-1} and ~1695 cm^{-1}, indicating the formation of β-sheets. This transformation from α-helix to β-sheet corresponds with the aggregation of Aβ peptides into fibrils. Additionally, the spectra initially displayed a peak at ~1545 cm^{-1}, indicative of α-helical structures, which gradually diminished, aligning with the structural transition observed in the Amide I region. Peaks corresponding to side chain motions and other functional groups (e.g., CH_2 and CH_3 bending vibrations) exhibited slight shifts, reflecting changes in the local environment as aggregation proceeded. The FTIR analysis of the RuIII complex revealed distinct absorption peaks, validating its molecular structure. The spectrum displayed strong bands around 500–600 cm^{-1} for Ru-Cl stretching vibrations and 400–450 cm^{-1} for Ru-O stretching vibrations.

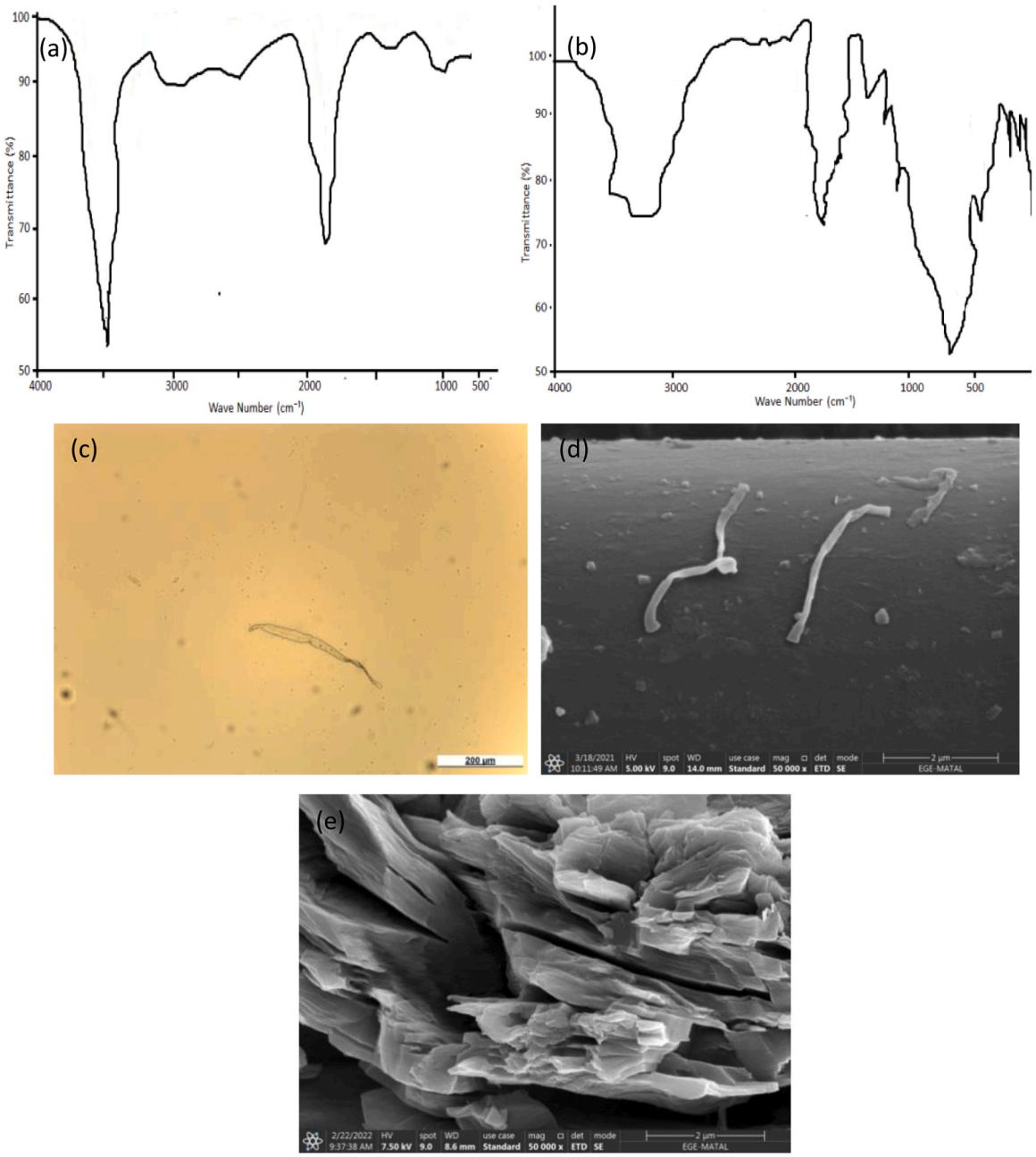

Fig. 1. illustrates various analyses and imaging of Amyloid Beta Peptide (ABP) and Ruthenium III (Ru III): (a) the FTIR analysis of Amyloid Beta Peptide (ABP), which identifies the characteristic functional groups and their interactions; (b) the FTIR spectrum of Ruthenium III (Ru III), detailing its unique vibrational modes; (c) the fluorescence spectroscopy image of Amyloid Beta Peptide (ABP), showing its emission properties and fluorescence behavior; (d) the HRSEM image of Amyloid Beta Peptide (ABP), providing high-resolution surface morphology; and (e) the HRSEM picture of Ruthenium III, displaying its detailed structural features at the chemical element.

These results align with the anticipated vibrational modes for RuIII chloride, confirming the successful synthesis and purity of the complex. Fluorescence microscopy allowed the observation of Aβ peptide aggregation, with the progression from faint staining to dense, fibrillar structures at later stages indicating the formation of β-sheet-rich amyloid fibrils (Fig. 1c). Fluorescence microscopy, particularly when combined with advanced imaging techniques, is a powerful tool for studying the surface morphology of amyloid beta plaques [14]. The self-assembly of Pro-Phe-Phe was studied using HRSEM, which revealed an extensive and unbranched helical fibre network topology. ABP (Fig. 1d) self-assembles into amyloid-like fibers when mixed with pH 7. Our design was inspired by the noncovalent interactions and distinctive motifs characteristic of amyloid protein aggregations. Incorporating strong Glu and Lys groups at the N and C termini of peptides increased electrostatic interactions, allowing for controllable self-assembly by controlled alterations. The hydrophobic regions of AIP-1 and AIP-2 promote aggregation through polar and π-π relationships, similar to those found in amyloid forms. Repetitive hydrogen bonding along fibril structures resulted in the development of stable nanofibers. These noncovalent bonds in our work are displayed in the self-assembly of peptide nanofibers, exhibiting amyloid-like structural nucleation properties [15]. Fig1e presents the FTIR spectra for the cationic RuIII complex. Experimentally discovered bands in the upper far-IR range (460–570 cm^{-1}) correspond to significant displacement Ru-C-O stretching phases, δ (Ru-C-O), which involves multiple or all carbonyl groups.

3.2. Characterization of ACD

The FTIR spectrum of ACD is shown in Fig. 2a. The IR spectra analysis matched the resolved structures or proposed models from other indirect methods, especially for complex 6. Broad diffusion bands observed in the 3384 cm^{-1} to 3234 cm^{-1} range are typical of O-H groups that function with intermolecular bonds of hydrogen, confirming the presence of ethanol and water molecules in the crystals. The spectra also exhibited multiple bands in the 3103–3064 cm^{-1} range, indicating the presence of C-H aryl groups. The bonding of the 2, 2′-bipyridine receptor was verified by the v (C═N) band located between 1571 and 1609 cm^{-1}. These values, which are considerably higher than those for ionic compounds, indicate a monodentate coordination form. The generating vibrations of the phenolic group, v(C-O), appear in the complex spectrum between 1233 cm^{-1} and 1253 cm^{-1}, proving the coordination of the salicylate ligands. A low-intensity band within the low-wavenumber area, as mentioned in the literature, is likely due to Ru-N valence vibrations [16].

Fig. 2b shows the TGA curves of ACD, which exhibit a three-step weight loss under a nitrogen environment. The first stage of decomposition occurs at 90–100 °C, resulting in a 10–13 % weight loss due to absorbed water. ABP ligands degrade between 110 °C and 225 °C, causing a 22–30 % weight loss due to the disintegration of the amino acid ring. In the second stage, the Ru III decomposes between 250 °C and 300 °C, with a 48–56 % weight loss. Ruthenium (III) complexes remain stable at 300 °C. The results of the HRSEM cross-sectional thickness investigation of these ACD complexes are shown in Fig. 2c. For consistent Ru growth, all data points should exhibit a linear relationship. Our study found that only data points with significant sample thicknesses could be approximated with straight lines. The uniformity of the ACD, derived from a blend of ABP, Ru, and nivolumab (Opdivo), was evident.

The linear link between sample thickness and constant Ru development found in your study resembles recent discoveries in the field of nanocomposite materials. Researchers have underlined the necessity of sample thickness in maintaining homogeneous development of metal-based complexes. For instance, Sanjeev et al. [17] found that increasing sample thickness in Ru-based nanomaterials improved growth uniformity and crystallization, leading to more predictable and stable drug release patterns. Similarly, Torrente-López et al. [18] stated that achieving homogeneity in complex blends, such as the combination of ABP, Ru, and medicinal compounds like nivolumab (Opdivo), is crucial for assuring consistent material qualities. The representative HRSEM image of ABP-RuIII-NB displayed its fibrous structure and smooth texture characteristics. The primary benefits of utilising like fibrous structures effective carrier drugs include enhanced high susceptibility, cellular uptake, and ease of impact. These ACD offer an enhanced surface region, facilitating greater drug incorporation capacity and a controlled, slower rate of diffusion [19].

3.3. Drug release study

To utilize ABP-RuIII-NB (ACD) for cancer cell recovery, it is important to investigate given its focusing of NB within the sample can be maintained over a specific time. Approximately 81 % of NB was efficiently encapsulated within the ABP-Ru. Fig. 3 depicts the in vitro release structure of NB, which occurs in two different stages. The first delivery stage, caused by the release of surface-embedded NB, survived up to 10 h. This was promptly followed by a steady release of NB from the ABP-Ru that lasted up to 40 h. In a buffer environment, NB may gradually degrade and develop pores on its surface, facilitating long-

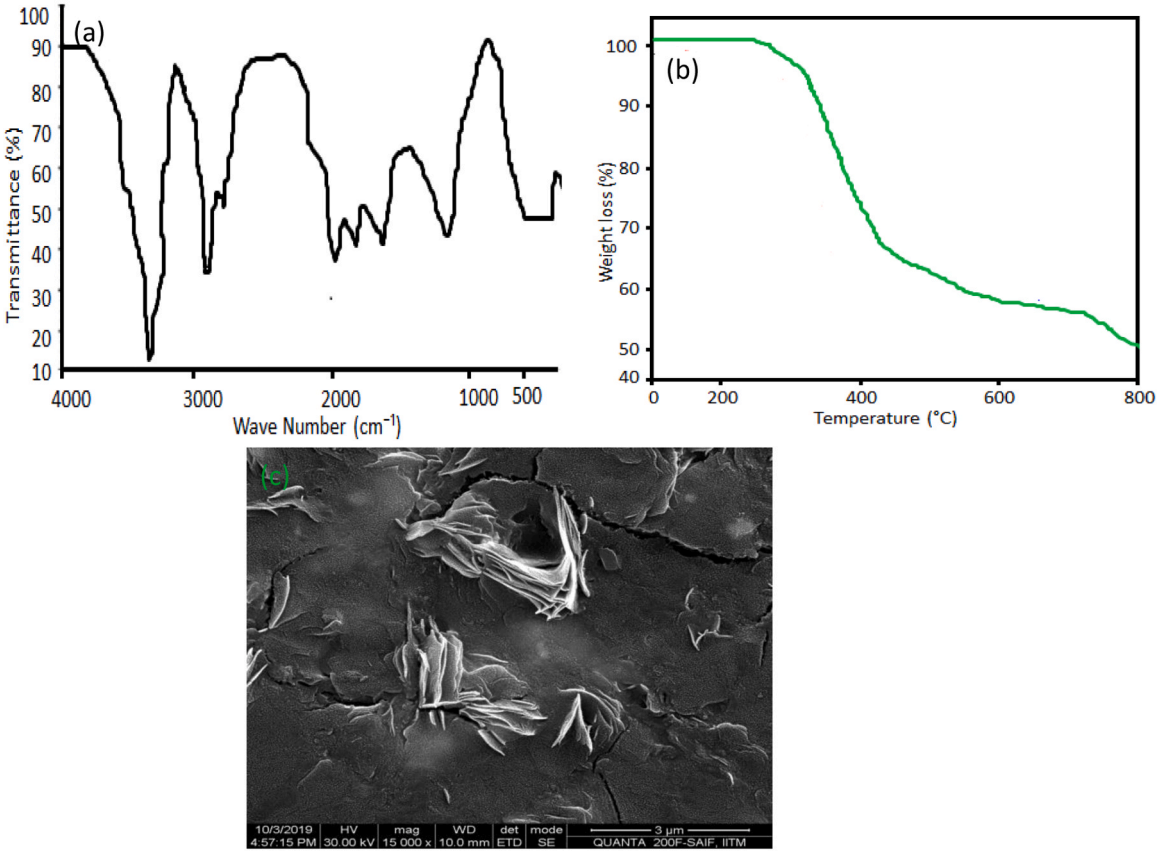

Fig. 2. presents the comprehensive characterization of the ABP-RuIII-NB (ACD) conjugate: (a) the FTIR spectra of ABP-RuIII-NB (ACD), identifying the specific functional groups and their interactions within the conjugate; (b) the TGA analysis of ABP-RuIII-NB (ACD), demonstrating its thermal stability and decomposition profile; and (c) the HRSEM image of ABP-RuIII-NB (ACD), revealing the detailed surface morphology and structural features of the conjugate at high resolution.

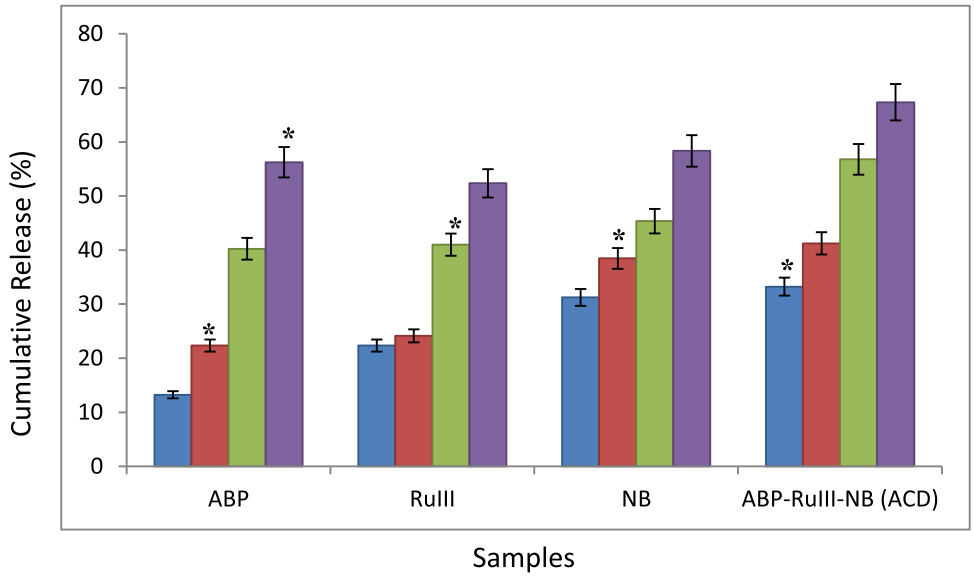

Fig. 3. depicts the drug release study, showcasing the release profiles of Amyloid Beta Peptide (ABP), Ruthenium III (RuIII), NB, and the ABP-RuIII-NB (ACD) conjugate, highlighting the comparative release rates and efficiency of each component as well as the combined conjugate over time.

term diffusion.

The two-stage release profile of NB encapsulated within ABP-RuIII-NB (ACD) is consistent with recent improvements in cancer-targeting drug delivery systems. Studies on nanoparticle-based drug carriers have demonstrated the need to attain both immediate and sustained drug release to improve therapeutic efficacy. Chehelgerdi et al. [20] demonstrated that a comparable two-phase release in nanocomposite structures might efficiently target cancer cells by first providing a high concentration of medicines to trigger apoptosis, followed by a protracted release that minimizes tumor reoccurrence. Furthermore, your observations of NB degradation in a buffer environment are comparable with those of Govindasamy et al. [21], who showed that drug-loaded nanoparticles exhibited surface erosion and pore formation, allowing for long-term drug diffusion. This gradual release is necessary to

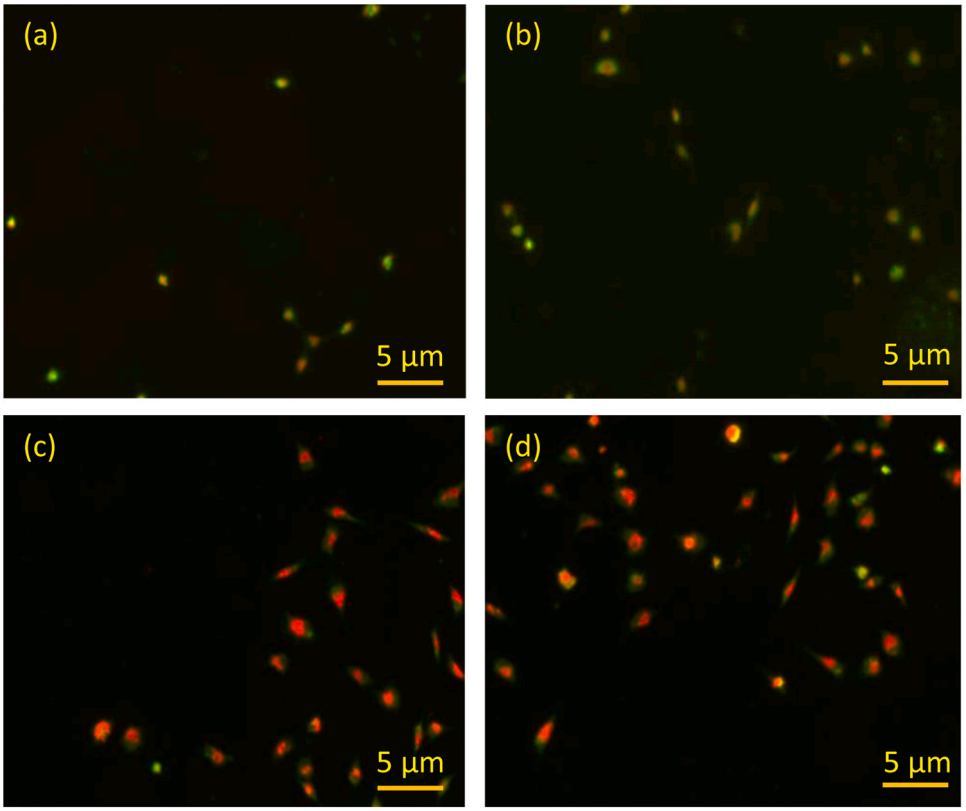

Fig. 4. illustrates the live/dead staining assay results for cells treated with different compounds: (a) Amyloid Beta Peptide (ABP), (b) Ruthenium III (RuIII), (c) NB, and (d) the ABP-RuIII-NB (ACD) conjugate, showing the viability and cytotoxic effects on cells with each treatment, where live cells are typically stained green and dead cells are stained red.

maintain therapeutic concentrations over long periods of time, improve pharmaceutical absorption, and reduce the danger of systemic toxicity. These findings highlight the significance of ABP-RuIII-NB's ability to balance rapid and sustained release for effective cancer therapy.

3.4. Invitro study

The cytotoxic potential of ABP, RuIII, NB, and ABP-RuIII-NB (ACD) was investigated using acridine orange (AO) and ethidium bromide (EB) differential staining techniques. The technique is based on membrane integrity changes, which alter cellular permeability to EB and AO dyes. AO is a nonspecific dye that can penetrate any cell membrane, staining both healthy and dead cells. In contrast, EB only stains dead cells with compromised tissue stability. A mixture of the two dyes is commonly used to visualise the production of dead cells. The cells stained are classified as live (green fluorescence), apoptotic bodies resulting from nuclear shrinkage and blebbing (moderate green to orange fluorescence), or dead cells (red fluorescence). In this investigation, cells treated to ABP-RuIII-NB exhibited a significant increase in the number of dead cells, with condensed nuclei that stained intensely with NB (Fig. 4). Cells treated with ABP-RuIII-NB also demonstrated notable morphological changes, such as tissue blebbing and the production of dead cells, which are characteristic features of apoptosis [22,23].

The morphological alterations observed in cells treated with ABP-RuIII-NB, such as tissue blebbing and the generation of dead cells, are classic signs of apoptosis, consistent with earlier research on apoptosis-inducing medicines. Apoptosis, defined by cell shrinkage, membrane blebbing, and DNA fragmentation, is a well-known side effect of effective anticancer therapy. Wilke et al. [24] discovered that ruthenium-based complexes, such as ABP-RuIII-NB, trigger apoptosis in cancer cells by producing reactive oxygen species (ROS), which causes mitochondrial malfunction and activation of caspase-dependent pathways. Senthil has [25] shown that nanoparticles containing therapeutic drugs such as nivolumab induce immune-mediated apoptotic responses, which enhances the cancer cell-killing efficacy. These morphological changes verify ABP-RuIII-NB's apoptotic efficacy, indicating that it has the potential to be a powerful agent in targeted cancer therapy by combining the apoptotic effects of the ruthenium complex and nivolumab.

The cell line used in these investigations is particularly relevant since it closely resembles the biological properties and behaviour of the target tissue or disease model. This cell line expresses specific markers and molecular pathways that are indicative of the condition under investigation, such as the development of amyloid beta peptides or sensitivity to metal-based chemotherapeutics like Ruthenium III. Furthermore, this cell line is well-documented and frequently used in scientific research examining medication efficacy, cytotoxicity, and mechanisms of action, assuring that the results are credible, reproducible, and can be correlated to in vivo settings. Using this specific cell line, the potential therapeutic advantages and cellular interactions of the ABP-RuIII-NB (ACD) compound can be assessed more accurately.

4. Conclusion

This study effectively synthesized and evaluated ABP-RuIII-NB (ACD) as a promising anticancer complex medication, demonstrating its potential for targeted cancer therapy. FTIR spectroscopy confirmed the complex's structural integrity and molecular interactions, while HRSEM gave information about its fibrous architecture and TGA showed thermal stability and disintegration patterns. Nivolumab was successfully encapsulated within the ABP-RuIII-NB complex, resulting in a 15-day controlled release profile. Cytotoxicity studies demonstrated that ABP-RuIII-NB causes considerable apoptosis in cancer cells, as evidenced by membrane blebbing and the development of apoptotic bodies. These findings emphasize the therapeutic potential of ABP-RuIII-NB in providing powerful anticancer effects via a sustained-release strategy. Future research will concentrate on optimizing medication dosage, improving drug release profiles, and assessing the complex therapeutic efficacy through in vivo experiments to determine its suitability in cancer treatment.

Authors' contribution

Rethinam Senthil – Methodology, Characterization, Formal analysis, writing the original draft and revision.

CRediT authorship contribution statement

Rethinam Senthil: Writing – review & editing, Writing – original draft, Visualization, Methodology, Formal analysis, Data curation, Conceptualization.

Declaration of Competing Interest

The authors declare that they have no known competing financial interests or personal relationships that could have appeared to influence the work reported in this paper.

Data availability

Data will be made available on request.

References

[1] M. Imbesi Bellantoni, G. Picciolo, I. Pirrotta, N. Irrera, M. Vaccaro, F. Vaccaro, F. Squadrito, G. Pallio, Oral cavity squamous cell carcinoma: an update of the pharmacological treatment, Biomedicines 11 (2023) 1112.
[2] K. Rekha, B. Venkidasamy, R. Govindasamy, M. Neralla, M. Thiruvengadam, Isothiocyanates (AITC & BITC) bioactive molecules: therapeutic potential for oral cancer, Oral Oncol. 133 (2022) 106060.
[3] V. Sankar, Y. Xu, Oral complications from oropharyngeal cancer therapy, Cancers (Basel) 15 (2023) 4548.
[4] S.Y. Lee, C.Y. Kim, T.G. Nam, Ruthenium complexes as anticancer agents: a brief history and perspectives, Drug Des. Dev. Ther. 14 (2020) 5375–5392.
[5] Q. Sun, Y. Li, H. Shi, Y. Wang, J. Zhang, Q. Zhang, Ruthenium complexes as promising candidates against lung cancer, Molecules 26 (2021) 4389.
[6] S. Adhikari, P. Nath, A. Das, A. Datta, N. Baildya, A.K. Duttaroy, S. Pathak, A review on metal complexes and its anti-cancer activities: recent updates from in vivo studies, Biomed. Pharmacother. 171 (2024) 116211.
[7] D. Karati, S. Meur, S. Mukherjee, S. Roy, Revolutionizing anticancer treatment: Ruthenium-based nanoplatforms pave new paths, Coord. Chem. Rev. 519 (2024) 216118.
[8] R. Senthil, S. Srividya, A.W. Aruni, B. Bhari, Jyotsna, T. Rajendren, Characterization of changes due to pH variation in beta peptide (25-35) leading to Alzheimer's disease, Int. J. Pept. Res Ther. 26 (2020) 1863–1870.
[9] F.K. El-Baz, G.A. Abdel Jaleel, R.A. Hussein, D.O. Saleh, *Dunalialla salina* microalgae and its isolated zeaxanthin mitigate age-related dementia in rats: modulation of neurotransmission and amyloid-β protein, Toxicol. Rep. 8 (2021) 1899–1908.
[10] J.C. Barrett, J.L. LaBelle, M. Tirrell, Self-assembling peptide-based building blocks in medical applications, Adv. Drug Deliv. Rev. 110-111 (2017) 65–79.
[11] A. Caporale, S. Adorinni, D. Lamba, M. Saviano, Peptide–protein interactions: from drug design to supramolecular biomaterials, Molecules 26 (2021) 1219.
[12] S. Acharya, F. Dilnawaz, S.K. Sahoo, Targeted epidermal growth factor receptor nanoparticle bioconjugates for breast cancer therapy, Biomater 30 (2009) 5737–5750.
[13] S.W. Vedakumari, R. Senthil, S. Sekar, C.S. Babu, T.P. Sastry, Enhancing anti-cancer activity of erlotinib by antibody conjugated nanofibrin - in vitro studies on lung adenocarcinoma cell lines, Mater. Chem. Phys. 224 (2019) 328–333.
[14] Z. Luo, H. Xu, L. Liu, T.Y. Ohulchanskyy, J. Qu, Optical imaging of beta-amyloid plaques in Alzheimer's disease, Biosensors (Basel) 11 (2021) 255.
[15] G. Wei, Z. Su, N.P. Reynolds, P. Arosio, I.W. Hamley, E. Gazit, R. Mezzenga, Self-assembling peptide and protein amyloids: from structure to tailored function in nanotechnology, Chem. Soc. Rev. 46 (2017) 4661–4708.
[16] M. Schoeller, M. Piroš, M. Litecká, K. Koňariková, F. Jozefíková, A. Šagátová, E. Zahradníková, J. Valentová, J. Moncol, Bipyridine Ruthenium(II) complexes with halogen-substituted salicylates: synthesis, crystal structure, and biological activity, Molecules 28 (2023) 4609.
[17] S. Gautam, I. Lakhanpal, L. Sonowal, N. Goyal, Recent advances in targeted drug delivery using metal-organic frameworks: toxicity and release kinetics, Nanotechnol 3-4 (2023) 100027.

[18] A. Torrente-López, J. Hermosilla, A. Salmerón-García, J. Cabeza, N. Navas, Comprehensive analysis of nivolumab, A therapeutic Anti-Pd-1 monoclonal antibody: impact of handling and stress, Pharmaceutics 14 (2022) 692.
[19] S. Gelperina, K. Kisich, M.D. Iseman, L. Heifets, The potential advantages of nanoparticle drug delivery systems in chemotherapy of tuberculosis, Am. J. Respir. Crit. Care Med 172 (2005) 1487–1490.
[20] M. Chehelgerdi, O.Q.B. Allela, R.D.C. Pecho, N. Jayasankar, D.P. Rao, T. Thamaraikani, M. Vasanthan, P. Viktor, N. Lakshmaiya, M.J. Saadh, A. Amajd, M.A. Abo-Zaid, R.Y. Castillo-Acobo, A.H. Ismail, A.H. Amin, R. Akhavan-Sigari, Progressing nanotechnology to improve targeted cancer treatment: overcoming hurdles in its clinical implementation, Mol. Cancer 22 (2023) 169.
[21] R. Govindasamy, R. Vaishnavi, S. Singh, M. Govindarasu, S. Sabura, K. Rekha, V. D. Rajeswari, S.S. Alharthi, M. Vaiyapuri, R. Sudarmani, et al., Green synthesis and characterization of cobalt oxide nanoparticles using *Psidium guajava* leaves extracts and their photocatalytic and biological activities, Molecules 27 (2022) 5646.
[22] A. Saraste, K. Pulkki, Morphologic and biochemical hallmarks of apoptosis, Cardiovasc. Res. 45 (2000) 528–537.
[23] S. Sagar, P. Ramani, S. Rajeshkumar, S. Gheena, Evaluation of antioxidant and anti-inflammatory effects Of 1,25 dihydroxycholecalciferol formulation- an in vitro study, J. Popul Ther. Clin. Pharmacol. 30 (2023) 247–253.
[24] N.L. Wilke, H. Burmeister, C. Frias, I. Ott, A. Prokop, Ruthenium Complex HB324 induces apoptosis via mitochondrial pathway with an upregulation of harakiri and overcomes cisplatin resistance in neuroblastoma cells in vitro, Int. J. Mol. Sci. 24 (2023) 952.
[25] R. Senthil, Recent development in fibrin nanoparticles (F-NPs) and in vitro study targeting of oral cancer, Nat. Prod. Res. 20 (2024) 1–3.